Effects and Mechanism of the Conditions of Sintering on Heavy Metal Leaching Characteristic in Municipal Solid Waste Incineration Fly Ash

Sheng He
Guangxi University College of Civil Engineering and Architecture
Yitong Zhou
Guangxi University College of Civil Engineering and Architecture
Peng Yu (py@gxu.edu.cn)
Guangxi University https://orcid.org/0000-0002-0735-3867
Xin Xia
Guangxi University College of Civil Engineering and Architecture
Hongtao Yang
Guangxi University College of Civil Engineering and Architecture

Research Article

Keywords: MSWI, Fly ash, Heavy metal, Leaching, Sintering, Grain size, Fluxing agent, Setting temperature

Posted Date: March 29th, 2022

DOI: https://doi.org/10.21203/rs.3.rs-1441273/v1

Abstract

Municipal solid waste incineration (MSWI) fly ash treated with toxicity metals holds enormous potential for constructure use to economize on resources and protect environment. To reach the goal, this study investigated the effects of sintering conditions on leaching characteristic of heavy metals for MSWI fly ash, especially Cr, Cr^{6+}, Ag, and Ba, with orthogonal and Box-Benhnken design experiment, which considered grain size (D_{50}=30, 45, and 60μm), fluxing agent (CaO=0, 2.5, and 5%), setting temperature (1000, 1050, and 1100℃), and setting time (120, 180, and 240min). The mechanism of immobilization for heavy metals was also discussed through the analyses of morphological characterizations, mineral phases, chemical composition and leaching values of metals. The results indicated that changing grain size and adding fluxing agent of CaO has positive influence on reducing the leaching of heavy metals compared with direct sintering. The leaching values of As, Pb, Cd, Cu, Ni, Zn, Mn, Hg, Be, Se and fluoride are not detected after sintering. Ideal sintered condition with desirability of 1.00 was predicted and optimized by Box-Benhnken response method in grain size of D_{50}=30μm, fluxing agent of CaO=5%, setting temperature=1050℃, and setting time=180min, which immobilized Cr, Cr^{6+}, Ag, and Ba lower than the limitation of standards. Actual experiment was consistent with numerical optimization. Furthermore, the model of leaching characteristic for heavy metals in MSWI fly ash was established to better explain the mechanism during sintering.

1. Introduction

Incineration power generation plays a crucial role in municipal solid waste disposal structure. In China, the throughput of **municipal solid waste incineration** (MSWI) for harmlessness was 897,700t per day, and the removal efficiency was 99.32% up to the end of 2020 as shown in China Ecological and Environment Bulletin, 2020. In the technological process of MSWI power plant as seen in Fig.1, waste is burned in incinerator, meanwhile chemical energy is converted into electric energy, which contains a large quantity of fly ash from the flue gas purification and heat recovery system, accounting for 3-5% of the waste(Ji et al. 2022). The main components of fly ash includes CaO, Cl, Na_2O, K_2O, SO_3, SiO_2, and Al_2O_3(Luan et al. 2016), in the present, considered as a substitute for a part of the cement binder. According to the research data, fly ash without treatment is used in mortar constitutes 5% of cement showing a greater compressive strength(Kirkelund et al. 2016). The proportioning of special concrete with fly ash is up to 20% in compressive strength of 43.73MPa(Turuallo and Mallisa 2018). Besides, dosage of fly ash in 30% as cement mixed in concrete was found that cementitious materials are generated leading to increasing of compressive strength(Zeng et al. 2020). However, MSWI fly ash is also an acknowledged hazardous waste formulated in Directory of National Hazardous Wasted (Version 2021) , causing harm to environment, human body, and the ecosystem due to the enriched in soluble chloride(Čarnogurská et al. 2015; Xu et al. 2022), some leaching of heavy metals, such as Cd, Pb, Cr, and Zn(Alorro et al. 2009; Kirk et al. 2002; Mangialardi 2001; Mangialardi et al. 1999), and persistent toxic organic compounds, such as PAH, and PCDD/Fs(Min et al. 2018).

Consequently, to make the industrial waste more acceptable and keep resource conservation, treatment measure must be taken for MSWI fly ash in construction use. Different methods have been developed, including washing(De Casa et al. 2007; Qiu et al. 2019; Wang et al. 2016), chemical stabilization(Ma et al. 2019; Wang et al. 2015), and thermal treatment(Fujii et al. 2019; Ma et al. 2017; Peng et al. 2020). Several studies about the treatment have been performed in construction resource utilization and environmental coordination. Some sources indicated that fly ash under washing used in mortar helps to increase compressive strength compared with traditional mortar(Bie et al. 2016; Keppert et al. 2015). Melting is utilized in MSWI fly ash for producing clinker of Alinite cement(Wu et al. 2012,2012)and Calcium Sulfoaluminate cement(Guo et al. 2014).

To date, high temperature sintering as a way of thermal treatment has been regarded as one of the most effective measures for stabilizing harmful materials of MSWI fly ash. However, the effect about stabilization of sintering usually suffers from many factors, such as temperature, time, grain size, and fluxing agent. The solidification conditions are variant in heavy metals. Moreover, fewer efforts were made to illuminate the sintering mechanism and realistic prediction which is critical to get deeper insight into contaminant transport.

In this work, the migration and transition behavior of heavy metals for MSWI fly ash during the high temperature sintering process were investigated, and a series of experiments were carried out: a) to work over the effects of grain size, fluxing agent, setting temperature, and setting time on the chloride's distribution, and leaching of heavy metals; b) to explore the optimum sintering conditions for the leaching of heavy metals lower than the limitation of standard during the sintering process; c) to probe into the

sintering and immobilization mechanism of chloride and heavy metals by characterizing crystalline phases, leaching concentration, and phase transformation. This study was expected to further understand the heavy metals existence form and transition behavior during the multiple factors sintering treatment process.

The rest of this paper is organized as follows: The materials, methods, and theory were introduced in Section 2. Morphological characterizations, chemical composition, mineral phase and leaching of heavy metals analyses with orthogonal and Box-Benhnken experiment for raw and sintered fly ash were discussed in Section 3. The model for sintering mechanism was established in Section 4. The conclusion was drawn in Section 5.

2. Material And Method

2.1. Materials

The raw samples used for study were MSWI fly ash collected from Baiyun Waste Incineration Plant in Guangzhou, Guangdong. The Grain size distribution curves of fly ash in different ball milling time without grinding aid is shown in Fig.2. Fly ash can be classified as ML (silt with low liquidity) according to Standard for Engineering Classification of Soil, and is made up of spherical and smooth particles with D_{50} of 60μm and small pores. It also shows that ball milling makes no difference on grain size of fly ash after 45s. The achievable minimum grain size of D_{50} by dry grinding is 30μm. As shown in Table 1, the primary chemical constituents of fly ash are noteworthy that, CaO, SiO_2, Na_2O, and K_2O take up about 60% jointly, yet SO_3 and Cl contents are over 30%. The chemical of CaO as fluxing agent in form of pellets with its analytical grade was purchased from a supplier of chemicals and reagents in Jiaxing, Zhejiang.

Table 1Chemical composition of raw fly ash for experiment(mass,%)

	SiO_2	Fe_2O_3	Al_2O_3	CaO	MgO	Na_2O	K2O	SO_3	Cl	P_2O_5	TiO_2	Other
FA1	4.477	1.467	1.581	42.319	1.699	9.497	5.721	7.499	21.525	1.378	0.953	1.884
FA2	4.808	1.816	1.028	41.547	0.086	7.013	6.79	6.99	26.503	0.266	1.337	1.816
FA3	2.168	1.56	1.102	45.58	1.132	7.359	6.562	5.772	25.431	0.559	0.897	1.878

Note:FA in different numbers indicates that fly ash is collected in different dates.

2.2. Solid-state sintering theory

The solid-state sintering is a method of powder densification under high temperatures without melting by proving surface energy and grain-boundary energy, including physical and chemical transformation. The production of crystal phase is the key to sintering(Wang et al. 2022). The theory of enhancing driving force and forcing atomic motion of powders in sintering for crystallization were used when designing experiment. The chlorine and heavy metals can be surrounded firmly by other atoms after sintering theoretically(Bordia and Olevsky 2009; Kang 2005).

In this work, solid-state sintering of MSWI fly ash was affected by setting temperature, setting time, grain size of fly ash, and dosage of fluxing agent. Changing grain size of fly ash could be a pre-treatment to alter granular surface regularity and surface energy by ball milling. The other hand, ball milling is conducive to lattice defect by crushing and extrusion on fly ash with energy storage. The setting time and setting temperature was related to the diffusion process of atoms in fly ash, influencing the effect of crystallization. Fluxing agent was used to change temperature and efficiency of sintering, and to diversify condition of crystalline phase.

2.3. Orthogonal and Box-Benhnken experiment methods

In this study, all the experiments for MSWI fly ash were performed according to the orthogonal and Box-Benhnken design. Four factors were to be considered in this work, which were grain size of fly ash, dosage of fluxing agent, setting temperature, and

setting time. To optimize the test, orthogonal test was applied to preliminary find out the effects of the four factors on content of chloride and the leaching of heavy metals, to provide a series of detection guiding for sintering mechanism and process, and to identify some heavy metals whose leaching value tending to zero or being far below standards(Geramita and Seberry 1979). Box-Benhnken response surface design was applied to analyze the influence of the four factors on leaching characteristic for subsequent analysis of residual heavy metals and chlorine, and to predict the optimal value and the corresponding conditions for the test.

According to the orthogonal tables, four factors were to be considered in three level. $L_9(3^4)$ orthogonal table was applied in this paper shown in Table 2. The sintering temperature is 0.8-0.9 times that of melting temperature of materials(Marfunin 1979). In addition, the sintering setting temperature was considered: 1000℃, 1050℃, or 1100℃ with a heating rate of 10℃/min. The raw fly ash was heated with setting time (120, 180, or 240min) at the target temperature. Grain size was concentrated in D_{50} of 30, 45, or 60μm by the method of dry ball-milling. The pellets of CaO were chosen as fluxing agent with the ratio of 0, 2.5, or 5%, by considering the effect of chemical composition of fly ash.

Table 2 Orthogonal experiment design of $L_9(3^4)$

No.	Factor			
	Grain size of D_{50}(μm)	Dosage of fluxing agent(%)	Setting temperature(℃)	Setting time(min)
S1	60	0	1000	120
S2	45	0	1050	180
S3	30	0	1100	240
S4	60	2.5	1050	240
S5	45	2.5	1100	120
S6	30	2.5	1000	180
S7	60	5	1100	180
S8	45	5	1000	240
S9	30	5	1050	120

When it comes to Box-Benhnken response surface table, a total of 27 experiments with four variables at three different levels were used, which were chosen as the same as orthogonal design. It can be seen from the Table 3 that three center points per block was adopted in the test.

Table 3 Box-Benhnken experiment design

Numeric	Name	Units	Low	High
A	Grain size of D_{50}	μm	30	60
B	Dosage of fluxing agent	%	0	5
C	Setting temperature	℃	1000	1100
D	Setting time	min	120	240

The raw sample of MSWI fly ash were dried in electric drying oven at 105℃ for 8h. The dried powder was ground in Planetary Ball Milling (JC-QM, Guangxi University) to the target of Grain size, and then mixed with CaO in alumina crucible for sintering. The process of sintering was in Muffle Furnace (SX2-10-12A, Guangxi University).

2.4. Testing methods

2.4.1. Grain-size test

To explore a target field of grain size of fly ash in different time under dry-ball milling, laser particle size analyzer (MAZ3000, Malvern, UK) was carried out for the samples with various ball milling time (0, 15, 25, 30, 45, or 60s) in 400 r/min. The samples were measured by the theory of Michelson and Franhoff.

2.4.2. Morphology characterization

The mineral structure, crystallinity, and phase transformation of raw fly ash and sintered fly ash were identified **X-ray diffraction** (XRD) (Ultima IV, Rigaku, Japan). They were analyzed over a range of 10-80° (2θ) at the scanning speed of 4°/min. The measured results were identified by comparing with the standard powder diffraction database of the International Centre for Diffraction Data (ICDD PDF-2 Release 2008). The microstructure of fly ash was observed by **scanning electron microscopy** (SEM) (S-3400N, Hitachi, Japan). The chemical composition of fly ash was measured by **X-ray fluorescence** (XRF) (S8 TIGER, Bruker, German).

2.4.3. heavy metals leaching characteristics test

The leaching characteristics of fourteen heavy metals were analyzed conforming to Solid Waste-Extraction Procedure for Leaching Toxicity-Sulphuric Acid& Nitric Acid Method HJ/T 299, CN. Extraction liquid was used in pH 3.2 as a leaching solution. The samples were soaked for 18h with liquid/solid ratio of 10 mL/g. The leaching concentrations of heavy metals were measured by Inductively Coupled Plasma-Atomic Emission Spectrometry (ICP-AES) (5900 ICP-OES, Agilent, Australia).

3. Results And Discussions

3.1. Morphological characterizations analysis

The SEM results in Fig.3 of raw fly ash in three grain size of D_{50}(30, 45, or 60μm) supported the hypothesis of original experiment design that ball milling only change grain size and distribution by crushing and extrusion on fly ash without impacting on micromorphology. The results showed that the surface of raw fly ash particles is surrounded by flocculent and globosity with high porosity. The samples in Fig.4 of different grain size show that fly ash under ball milling is increased with bulk density. Particles change into powders from granules.

The samples of sintered fly ash are shown in Fig.5. Comparing with raw sample, it was observable that sintered fly ash bulk density grows up and the gap of particles is dropped. The color has noticeable change from gray to malachite green. It might be due to formation of new minerals. The external morphology of sintered fly ash was studied by SEM, as shown in Fig.6. The results revealed that treatment significantly affects the microstructure of the fly ash. Sintering causes particles to become lower porosity and to weld together forming a dense structure. In previous studies, sintered coal fly ash can be seen many small granular hydroxysodalite aggregates on the surface with SEM(Luo et al. 2018). Red mud-fly ash is formed a mass of bar-structure from spherical particles under sintering(Samal et al. 2015). After sintering, the spherical particles of coal fly ash disappeared(Wu et al. 2014). In addition, sintering leads to dramatic particles aggregation with bar or rod-shape in microstructure, as a result of formation and growth of crystal nucleus. The raised surfaces indicated that directional crystals grow at fracture. The upturn of crystallinity helps to improve bulk density and mechanical properties. The migration and motion rate of atomics build up by enhancing driving force during sintering.

3.2. Chemical composition and XRD analysis

The chemical compositions tested with XRF of raw fly ash and sintered fly ash under different condition in orthogonal design are given in Fig.7. It can be seen that CaO, SiO_2, Al_2O_3, SO_3 and Cl are the main compositions for sintered fly ash, which is notable differences with raw fly ash. The chemical compositions of sintered fly ash are under different group remain level. The content of CaO, SiO_2, and Al_2O_3 all increased to 50.16%, 11.96%, and 5.25% from 41.55%, 4.81%, and 1.03%, respectively. Sintering contributes to optimize compositions of fly ash for construction use as cement, because of more similar components. CaO is beneficial to the growth of crystal with high value. While, Na_2O, K_2O, and Cl for sintered fly ash were all lower than raw fly ash. Particularly, the

percentage of Cl nearly fell from 26.50% to 12.74%, which provides the evidence that sintering helps to reduce the content of Cl being harmful to cement(Chen et al. 2016).

Fig.8 demonstrates the XRD patterns of raw and sintered fly ash are under various orthogonal conditions. It was discerned that the main differences in the raw and sintered samples were the variation in mineral peak intensity. By comparison with raw fly ash, the relative contents of $CaCO_3$ and CaClOH declined and even disappeared as the results that $CaCO_3$ and CaClOH decomposing at high temperature during sintering. It can be well explained as the change of chemical composition on CaO and Cl. Whereas the peak intensity of $CaTiO_3$, MgO, and $Ca_{12}Al_{14}O_{33}$ increased or occurred. This phenomenon supports the analysis of SEM that crystallinity and intensity of the crystal phases increased in degree by sintering. $Ca_{12}Al_{14}O_{33}$ is created by the solid-state reaction with CaO and Al_2O_3(Rudradawong et al. 2020), which belongs to orthorhombic crystal with cyan-gray N*g* and blue-green N*p* surface, which is in good agreement with sintered fly ash images.

The content of soluble chloride salts as NaCl and KCl in sintered fly ash were reduced by 50% nearly comparing raw samples in Fig.8. Howerver, $Ca_5(PO_4)_3Cl$ raised practically four times under sintering. The results show that a part of Cl is immobilized as a stable mineral reducing the possibility of escaping. The other Cl is attached on the sintered fly ash particles as soluble chloride salts. Thus, sintering is limited to remove the whole Cl in this study, which may be taken off by washing for those soluble chloride salts.

Fig.9 shows the change for crystallinity of raw and sintered fly ash. The value with a mean of 89.78% under sintering, while raw fly ash only is 65.93%. this result provided specific evidence that the treatment in this study helps fly ash to improve the growing of crystals and reduce the leaching of heavy metals. It is worth notice that the value of group S8 is 99.99% which means a greatly tight structure in particles.

3.3. Leaching of toxicity metals analysis

The leaching performances of sintered fly ash were evaluated using toxicity threshold included in the standard of Identification Standards for Hazardous Wastes-Identification for Extraction Toxicity (GB5085.3-2007), Integrated wastewater Discharge Standard (GB8978-1996), and Technical Specification for Coprocessing of Solid Waste in Cement Kiln (GB30760-2014). All the results were summarized in Table 4. It is shown that leaching characteristic of toxicity elements in the most orthogonal samples are much lower than the standard limits. Specifically, the leaching values of As, Pb, Cu, Mn, Hg, Be, Se, and Fluoride were even not detected, indicating that proposed sintering methods have immobilization contribution on the most toxicity elements. In spite that the effects of sintering design have some limitations in reducing the leaching of, Cr, Cr^{6+} Ag, and Ba. In group S2 and S3, the immobilization of Cr is only 25.74% and 19.68%, respectively. Even the leaching of Cr^{6+} increased from 5.54 to 6.5mg/L. The result showed that As, Pb, Cd, Cu, Ni, Zn, Mn, Hg, Be, Se and fluoride barely indicate leaching characteristic in orthogonal test.

Table 4 Orthogonal test table for sintering experiment

No.	Leaching of toxicity metal elements(mg/L)														
	As	Pb	Cd	Cr	Cu	Ni	Zn	Mn	Hg	Cr^{6+}	Be	Ag	Ba	Se	Fluoride
FA	0.41	0.64	0.04	8.74	0.54	0.29	2.4	1.5	0.07	5.54	0.008	0.94	115	1.65	0.65
S1	ND	ND	0.01	2.93	ND	ND	ND	ND	ND	1.85	ND	0.62	13.45	ND	ND
S2	ND	ND	0.03	2.49	ND	ND	0.3	ND	0.02	2.5	ND	0.59	5.29	ND	ND
S3	ND	ND	0.02	3.15	ND	ND	0.02	ND	ND	1.45	ND	0.41	4.22	ND	ND
S4	ND	0.29	ND	0.38	ND	0.12	0.01	ND	ND	1.612	ND	0.28	34.4	ND	ND
S5	ND	ND	0.02	0.68	ND	ND	0.01	ND	ND	0.323	ND	0.18	10.72	ND	ND
S6	ND	ND	ND	0.89	ND	0.19	ND	ND	ND	0.78	ND	0.23	26.8	ND	ND
S7	ND	ND	0.03	0.26	ND	0.23	ND	ND	ND	0.289	ND	ND	33.3	ND	ND
S8	ND	ND	0.03	0.65	ND	0.18	ND	ND	ND	0.759	ND	0.36	38.3	ND	ND
S9	ND	ND	0.04	0.28	ND	0.22	ND	ND	ND	0.254	ND	0.16	39.7	ND	ND
ST	0.1	0.3	0.03	0.2	0.5	0.2	1	1	0.05	0.5	0.005	0.5	100	1	100

Note: ND Indicates not detected, ST Indicates Standard thresholds.

3.4. Response surface of Box-Benhnken analysis

The leaching of Cr, Cr^{6+}, Ag, and Ba were chosen to investigate with Box-Benhnken response surface method for further revealing the influence of four factors on above toxicity elements, and calculating optimal value and experiment design with sintered fly ash. It was considered that residual toxicity elements can be greatly restricted in crystal phase according to the results of orthogonal experiment. The findings as shown in Table 5 provide substantial evidence for four variables having a major impact on the immobilized toxicity metals.

Table 5 Heavy metals leaching of treated samples in Box-Benhnken experiment for Cr, Cr^{6+}, Ag, and Ba (mg/L)

No.	Factor				Leaching characteristics of heavy metals(mg/L)			
	Grain size of D_{50}(μm)	Dosage of fluxing agent(%)	Setting temperature(°C)	Setting time(min)	Cr	Ag	Ba	Cr^{6+}
1	45	5	1050	240	0.322	0.1	26.5	0.803
2	30	2.5	1100	180	1.08	0.091	19.8	0.834
3	45	0	1100	180	2.83	0.47	5.4	3.21
4	60	5	1050	180	0.165	0.16	39.2	0.345
5	60	2.5	1000	180	0.25	0.58	32.1	0.732
6	45	2.5	1100	120	0.56	0.22	25.6	1.32
7	60	2.5	1050	240	0.34	0.493	30.4	1.03
8	45	2.5	1050	180	0.446	0.312	30.4	0.476
9	45	5	1050	120	0.22	0.23	32.9	0.345
10	45	2.5	1050	180	0.435	0.451	29.4	0.443
11	60	2.5	1100	180	0.287	0.21	32.6	1.98
12	30	2.5	1000	180	0.82	0.57	27.5	0.367
13	45	5	1100	180	0.73	0.05	27.3	0.892
14	45	0	1000	180	2.1	0.72	6.87	2.26
15	45	2.5	1050	180	0.58	0.45	26.9	0.623
16	45	0	1050	240	2.49	0.66	3.6	2.9
17	60	0	1050	180	0.9	0.59	11.2	2.25
18	30	2.5	1050	240	0.764	0.222	24.1	0.786
19	60	2.5	1050	120	0.241	0.47	34.2	0.98
20	45	2.5	1000	120	0.598	0.56	27.9	0.562
21	45	5	1000	180	0.65	0.283	34.7	0.432
22	30	0	1050	180	3.123	0.621	7.9	1.65
23	45	0	1050	120	1.42	0.692	4.12	1.72
24	45	2.5	1000	240	0.61	0.554	28.3	0.98
25	30	2.5	1050	120	0.732	0.481	21.3	0.34
26	30	5	1050	180	0.2	0.148	33.2	0.423
27	45	2.5	1100	240	0.59	0.23	20.6	1.45

3.4.1. Effect of grain size

The experiment results were analyzed with ANOVA of grain size for model in Table 6, which indicates grain size has influence on the leaching of Cr, Ba, and Cr^{6+}. Since P-values less than 0.05 are significant yet values greater than 0.1 are not significant. Fig.10 is represented the regression model demonstrating the impact of grain size on toxicity metals when fluxing agent, setting temperature, and setting time is 2.5%, 1050°C, and 180min, respectively. It can be seen that Ag leaching remains level with grain size. However, Ba leaching was showed significant changes. The leaching of Ba, and Cr^{6+} increased as grain size up while Cr decreased steadily.

Table 6 ANOVA analysis of Box-Benhnken models for Cr, Cr^{6+}, Ag, and Ba with grain size of D_{50}

Source	Sum of Squares	Mean Square	F-value	P-value	
Cr	1.71	1.71	27.19	0.0002	significant
Ag	0.0114	0.0114	2.89	0.1033	not significant
Ba	175.57	175.57	50.75	< 0.0001	significant
Cr^{6+}	0.7091	0.7091	14.78	0.0023	significant

3.4.2. Effect of fluxing agent

Table 7 depicts that fluxing agent of CaO makes marked impression on immobilization of all toxicity metals in the experiment. As can be seen from the Fig.11, great changes have taken place in leaching of Ba, Cr, and Cr^{6+} with grain size, setting temperature, and setting time is D_{50}=45μm, 1050℃, and 180min, respectively. Surprisingly, Ba leaching sharply went up with content of CaO rising between 0 to 1%. Then, the rate of increase slow down after 1%. The situation nearly reached a peak of 4%. The adding of CaO as fluxing agent helps to immobilize Ag, Cr, and Cr^{6+}. But it is limited to Cr and Cr^{6+} in the number of 4.5% for CaO.

Table 7 ANOVA analysis of Box-Benhnken models for Cr, Cr^{6+}, Ag, and Ba with fluxing agent of CaO

Source	Sum of Squares	Mean Square	F-value	P-value	
Cr	9.32	9.32	147.81	< 0.0001	significant
Ag	0.645	0.645	163.28	< 0.0001	significant
Ba	1994.6	1994.6	576.54	< 0.0001	significant
Cr^{6+}	9.63	9.63	200.77	< 0.0001	significant

3.4.3. Effect of setting temperature

As is illustrated in the Table 8, setting temperature has influence on Ag, Ba, and Cr^{6+} leaching when grain size, fluxing agent, and setting time is D_{50}=45μm, 2.5%, and 180min, respectively. The tendency of heavy metals leaching is proved in Fig.12. Ag and Ba leaching were gradual decline in higher temperature which are in contrast to Cr^{6+}. Ba is the most sensitive to temperature.

Fig.13 is used to explore interaction between fluxing agent and setting temperature on Cr^{6+}, Cr, and Ba by 3D surface mode, which grain size of D_{50} is 45μm, and setting time is 180min. The leaching of Cr^{6+} and Cr showed an extreme influence on interaction rather than one factor. Therefore, it was decreased when adding dosage of CaO and receding the temperature at the same time. However, Ba leaching values were control with interaction approaching one factor for fluxing agent of CaO. The trends of change for three metals are similar.

Table 8 ANOVA analysis of Box-Benhnken models for Cr, Cr^{6+}, Ag, and Ba with setting temperature

Source	Sum of Squares	Mean Square	F-value	P-value	
Cr	0.0917	0.0917	1.45	0.2511	not significant
Ag	0.332	0.332	84.05	< 0.0001	significant
Ba	56.64	56.64	16.37	0.0016	significant
Cr^{6+}	1.58	1.58	32.92	< 0.0001	significant

3.4.4. Effect of setting time

Table 9 is clearly shown that setting time only has significant influence on immobilization of Cr^{6+} with grain size, fluxing agent, and setting temperature being D_{50}=45μm, 2.5%, and 1050℃, respectively. Fig.14 proves that high temperature has negative impact on immobilization of Cr^{6+}. Especially, Cr^{6+} leaching showed a steep growing after 1035℃.

Table 9 ANOVA analysis of Box-Benhnken models for Cr, Cr^{6+}, Ag, and Ba with setting time

Source	Sum of Squares	Mean Square	F-value	P-value	
Cr	0.1508	0.1508	2.39	0.148	not significant
Ag	0.0129	0.0129	3.27	0.084	not significant
Ba	13.06	13.06	3.78	0.0758	not significant
Cr^{6+}	0.5994	0.5994	12.5	0.0041	significant

Fig.15 is shown as the interaction of fluxing agent of CaO and setting time on Cr^{6+}, Cr, and Ba in 3D model when grain size of D_{50} and setting temperature are set up in 45μm, and 1050℃, respectively. The tendency is like the results of the interaction between fluxing agent and setting temperature. However, the trend for change of Cr and Cr^{6+} was slow down.

3.4.5. Optimal prediction analysis

The model condition was predicted response by desirability function in Box-Benhnken response surface. The leaching of heavy metals as functions were set for the goal under the standard limitation for numerical optimization, which was used to calculate the highest desirability and to design the subsequent experiment. In this work, the ideal selection focused on a desirability of 1.00, and the reduction of energy consumption. Thus, the optimal condition is grain size of D_{50}=30μm, fluxing agent of CaO=5%, setting temperature=1050℃, and setting time=180min, resulting in the leaching of Cr, Ag, Ba, and Cr^{6+} is 0.121, 0.131,30.25, and 0.266, respectively. The theoretical variables were compared with experiment in three tests with average results being shown in Table 10. The experimental results supported the theoretical optimization that the average is observed to be 0.129, 0.16, 31.51, and 0.23, respectively, which implies that Box-Benhnken response surface contributes to optimize the sintering process.

Table 10 Leaching of Cr, Cr^{6+}, Ag, and Ba in optimized and actual experiment (mg/L)

Toxicity metals	Optimal value	Experimental value in average
Cr	0.121	0.129
Ag	0.131	0.16
Ba	30.25	31.51
Cr^{6+}	0.266	0.23

3.5. Sintering mechanism of MSWI fly ash

The fly ash was treated with direct heating for sintering accumulating limited internal energy. Therefore, the results of crystallinity and solidification for toxicity metals was shown a low performance. crystal is formed in geometry as rules spontaneously when temperature up in a period by breaking bonds. Rising temperature provides thermal energy for internal motif to gain kinetic energy(Pan et al. 2020). The particles are formed from other aggregation structures to crystalline state, which storage the least internal energy and possess the most stable shape. At the same time, arrangement space is sharply reduced for whole atoms as the result of density decreasing as characterization. In addition, solid materials are transferred and interchanged due to the dual effects of physics and chemistry, exposing the shortage with an immediate heating.

In this study, the treatment of sintering was improved through adding two additional factors as the method to promote crystallization in fly ash and immobilization of heavy metals. The specific mechanism is shown in Fig.16 giving a rational

explanation for inherent change during treatment. Atoms keep moving with certain speed and distance in particles for fly ash. It is simple for toxicity metals to depart from particles when leaching. Changing grain size with ball milling was utilized to provide energy under the mechanical work for atoms and Irregular surface. Besides, it is useful to reduce the distance of particles(Luo et al. 2017). Fly ash has saved a large energy before sintering. CaO contributes to decrease melting point in SiO_2-CaO or SiO_2-Al_2O_3-CaO system as high-melting oxide(Zha et al. 2021). It is helpful to reach the sintered phase and reduce the energy for supporting the growth of crystal. Fluxing agent was used to shorten sintering time and reduce consumption. The results of sintering were considerable with previous treatment. Particles are push to a drastic motion as temperature growing. Mineral phases, such as $CaTiO_3$, and $Ca_{12}Al_{14}O_{33}$ are continuously generated at setting temperature and time, occupying a large space in particle. Toxicity metals are locked and surrounded by other crystals when particles compacted. Gigantic binding force becomes the limitation on leaching of metals.

The findings of this study were restricted to other factors that may contribute to sintering, for example, sintering atmosphere, and pressure. The leaching of As, Pb, Cd, Cu, Ni, Zn, Mn, Hg, Be, Se, and fluoride hardly was detected as the values being over the lowering. Thus, they were left out to consider the relation with setting temperature, setting time, grain size of fly ash, and dosage of fluxing agent. Besides, the findings did not imply the leaching characteristic for fly ash in the environment permanently.

4. Conclusion

In this study, the treatments of ball milling and sintering for MSWI fly ash were conducted to investigate the effect of grain size (D_{50}=30, 45, and 60μm), fluxing agent (CaO with 0, 2.5, and 5%), setting temperature (1000, 1050, and 1100℃), and setting time (120, 180, and 240min) on the leaching characteristic of toxicity metals, and to explore the mechanism of sintered fly ash under physical and chemical progresses. Transformation of apparent and microscopic morphology, distribution of particle size, chemical composition, crystallinity, changes of formation of minerals, and leaching values of heavy metals were tested and analyzed under different sintering experimental condition with orthogonal design and Box-Benhnken response method. The main findings are represented as follows:

a) Sintering contained ball milling and fluxing agent for MSWI fly ash is substantial agreement with original hypothesis from the experiment data. The growth of crystal in particles is connected and welded under sintering to reduce internal space and restrict the leaching characteristic of heavy metals. The average of crystallinity is 89.78% while raw fly ash in 65.93%, which causes the microscopic morphology transforming from smooth spherical or irregular flocculated to bar or rod-shape. The minerals of $CaTiO_3$, MgO, and $Ca_{12}Al_{13}O_{33}$ are formed with the mean of 10.6, 4.58, and 12.59%, respectively, proving the enhance of crystallinity, changing the samples color into malachite green, and enlarging the bulk density. The leaching values of As, Pb, Cd, Cu, Ni, Zn, Mn, Hg, Be, Se and fluoride are not detected, in addition that the most leaching of Cr, Ag, Ba, and Cr^{6+} are below the limitation after sintering and considerable with standards for construction use as hazardous waste.

b) Decreasing grain size with ball milling has a significant influence on restraining the leaching characteristic of Cr^{6+}, Ag, and Ba. It is utilized to provide energy for fly ash particles under the mechanical work for atoms and irregular surface. Fluxing agent of CaO is used to degrade the energy leading to sintered state by decreasing melting point in SiO_2-CaO or SiO_2-CaO-Al_2O_3 system. CaO also is seen as the main elements for crystallization during sintering, which is significant to reduce the leaching values of Cr^{6+}, Ag, and Cr as its rising. Since the burst of energy for atoms is determined to the quantity of energy absorbed during sintering. Setting time is shown less influence on leaching characteristic than setting temperature. Increasing temperature can be seen a positive influence on Ag and Cr, and negative influence on Cr^{6+} and Ba.

c) Based on the Box-Benhnken experiment, the ideal condition is predicted and optimized when considering grain size, fluxing agent, setting temperature, and setting time. In this selection, toxicity metals are limited under the standard in China, besides, time and resource costs are controlled in a lower level, which grain size of D_{50}=30μm, fluxing agent of CaO=5%, setting temperature=1050℃, and setting time=180min, is resulted in the leaching of Cr, Ag, Ba, and Cr^{6+} is 0.121, 0.131, 30.25, and 0.266, respectively. The experimental results are 0.129, 0.16, 31.51, and 0.23, respectively compared with theoretical optimization.

Declarations

Author contribution Sheng He: methodology, investigation, formal analysis, original draft writing, validation, building model, writing-review and editing; Yitong Zhou: data analysis, methodology, formal analysis, validation, writing-review and editing; Peng Yu: supervision, resources, funding acquisition, visualization. Xin Xia: building model, formal analysis, writing-review and editing; Hongtao Yang: building model, formal analysis, writing-review and editing.

Funding This work was supported by the Natural Science Foundation of China (51878786, 51738004), Research Grant for 100 Talents of Guangxi Plan, Starting Research Grant for High-level Talents from Guangxi University, Guangxi Major Research Program (AB19259013).

Data availability Not applicable

Ethics approval Not applicable.

Consent to participate Not applicable.

Consent for publication Not applicable.

Conflict of interest The authors declare no competing interests.

References

1. Alorro RD, Hiroyoshi N, Ito M, Tsunekawa M (2009) Recovery of heavy metals from MSW molten fly ash by CIP method Hydrometallurgy 97:8-14 doi:10.1016/j.hydromet.2008.12.007
2. Bie R, Chen P, Song X, Ji X (2016) Characteristics of municipal solid waste incineration fly ash with cement solidification treatment J Energy Inst 89:704-712 doi:10.1016/j.joei.2015.04.006
3. Bordia RK, Olevsky EA (2009) Advances in sintering science and technology Vol. American Ceramic Society ;Wiley,
4. Čarnogurská M, Lázár M, Puškár M, Lengyelová M, Václav J, Širillová = (2015) Measurement and evaluation of properties of MSW fly ash treated by plasma Measurement 62:155-161 doi:10.1016/j.measurement.2014.11.014
5. Chen Y, Gao J, Tang L, Li X (2016) Resistance of concrete against combined attack of chloride and sulfate under drying–wetting cycles Constr Build Mater 106:650-658 doi:10.1016/j.conbuildmat.2015.12.151
6. De Casa G, Mangialardi T, Paolini AE, Piga L (2007) Physical-mechanical and environmental properties of sintered municipal incinerator fly ash Waste Manage 27:238-247 doi:10.1016/j.wasman.2006.01.011
7. Fujii T, Kashimura K, Tanaka H (2019) Microwave sintering of fly ash containing unburnt carbon and sodium chloride J Hazard Mater 369:318-323 doi:10.1016/j.jhazmat.2018.12.114
8. Geramita CV, Seberry J (1979) Orthogonal designs Vol. M. Dekker,
9. Guo X, Shi H, Hu W, Wu K (2014) Durability and microstructure of CSA cement-based materials from MSWI fly ash Cement and Concrete Composites 46:26-31 doi:10.1016/j.cemconcomp.2013.10.015
10. Ji Z et al. (2022) Dioxins control as co-processing water-washed municipal solid waste incineration fly ash in iron ore sintering process J Hazard Mater 423:127138 doi:10.1016/j.jhazmat.2021.127138
11. Kang SL (2005) Sintering: Densification, Grain Growth and Microstructure Vol. A Butterworth-Heinemann Title,
12. Keppert M, Siddique JA, Pavlík Z, Černý R (2015) Wet-Treated MSWI Fly Ash Used as Supplementary Cementitious Material Adv Mater Sci Eng 2015:1-8 doi:10.1155/2015/842807
13. Kirk DW, Chan CCY, Marsh H (2002) Chromium behavior during thermal treatment of MSW fly ash J Hazard Mater 90:39-49 doi:10.1016/S0304-3894(01)00328-4
14. Kirkelund GM, Ottosen LM, Jensen PE, Goltermann P (2016) Greenlandic waste incineration fly and bottom ash as secondary resource in mortar International Journal of Sustainable Development and Planning 11:719-728 doi:10.2495/SDP-V11-N5-719-728
15. Luan J, Chai M, Li R (2016) Heavy Metal Migration and Potential Environmental Risk Assessment During the Washing Process of MSW Incineration Fly Ash and Molten Slag Procedia Environmental Sciences 31:351-360 doi:10.1016/j.proenv.2016.02.047

16. Luo Y, Ma S, Liu C, Zhao Z, Zheng S, Wang X (2017) Effect of particle size and alkali activation on coal fly ash and their role in sintered ceramic tiles J Eur Ceram Soc 37:1847-1856 doi:10.1016/j.jeurceramsoc.2016.11.032
17. Luo Y, Zheng S, Ma S, Liu C, Wang X (2018) Preparation of sintered foamed ceramics derived entirely from coal fly ash Constr Build Mater 163:529-538 doi:10.1016/j.conbuildmat.2017.12.102
18. Ma W et al. (2019) Performance of chemical chelating agent stabilization and cement solidification on heavy metals in MSWI fly ash: A comparative study J Environ Manage 247:169-177 doi:10.1016/j.jenvman.2019.06.089
19. Ma W, Fang Y, Chen D, Chen G, Xu Y, Sheng H, Zhou Z (2017) Volatilization and leaching behavior of heavy metals in MSW incineration fly ash in a DC arc plasma furnace Fuel 210:145-153 doi:10.1016/j.fuel.2017.07.091
20. Mangialardi T (2001) Sintering of MSW fly ash for reuse as a concrete aggregate J Hazard Mater 87:225-239 doi:10.1016/s0304-3894(01)00286-2
21. Mangialardi T, Paolini AE, Polettini A, Sirini P (1999) Optimization of the solidification/stabilization process of MSW fly ash in cementitious matrices J Hazard Mater 70:53-70 doi:10.1016/s0304-3894(99)00132-6
22. Marfunin CS (1979) Physics of minerals and inorganic materials Vol. Springer-Verlag,
23. Min Y, Liu C, Shi P, Qin C, Feng Y, Liu B (2018) Effects of the addition of municipal solid waste incineration fly ash on the behavior of polychlorinated dibenzo-p-dioxins and furans in the iron ore sintering process Waste Manage 77:287-293 doi:10.1016/j.wasman.2018.04.011
24. Pan X, Cui W, Zhang C, Yu H (2020) Formation kinetics and transition mechanism of CaO·SiO2 in low-calcium system during high-temperature sintering J Cent South Univ 27:3269-3277 doi:10.1007/s11771-020-4545-1
25. Peng Z, Weber R, Ren Y, Wang J, Sun Y, Wang L (2020) Characterization of PCDD/Fs and heavy metal distribution from municipal solid waste incinerator fly ash sintering process Waste Manage 103:260-267 doi:10.1016/j.wasman.2019.12.028
26. Qiu Q et al. (2019) Degradation of PCDD/Fs in MSWI fly ash using a microwave-assisted hydrothermal process Chinese J Chem Eng 27:1708-1715 doi:10.1016/j.cjche.2018.10.015
27. Rudradawong C, Kitiwan M, Goto T, Ruttanapun C (2020) Positive ionic conduction of mayenite cement Ca12Al14O33/nano-carbon black composites on dielectric and thermoelectric properties Materials Today Communications 22:100820 doi:10.1016/j.mtcomm.2019.100820
28. Samal S, Ray AK, Bandopadhyay A (2015) Characterization and microstructure observation of sintered red mud–fly ash mixtures at various elevated temperature J Clean Prod 101:368-376 doi:10.1016/j.jclepro.2015.04.010
29. Turuallo G, Mallisa H (2018) Using Cementitious Materials Such as Fly Ash to Replace a Part of Cement in Producing High Strength Concrete in Hot Weather IOP conference series. Materials Science and Engineering 316:12039 doi:10.1088/1757-899X/316/1/012039
30. Wang F, Zhang F, Chen Y, Gao J, Zhao B (2015) A comparative study on the heavy metal solidification/stabilization performance of four chemical solidifying agents in municipal solid waste incineration fly ash J Hazard Mater 300:451-458 doi:10.1016/j.jhazmat.2015.07.037
31. Wang X, Li A, Zhang Z (2016) The Effects of Water Washing on Cement-based Stabilization of MWSI Fly Ash Procedia Environmental Sciences 31:440-446 doi:10.1016/j.proenv.2016.02.095
32. Wang X, Zhu K, Zhang L, Li A, Chen C, Huang J, Zhang Y (2022) Mechanical property and heavy metal leaching behavior enhancement of municipal solid waste incineration fly ash during the pressure-assisted sintering treatment J Environ Manage 301:113856 doi:10.1016/j.jenvman.2021.113856
33. Wu K, Shi H, De Schutter G, Guo X, Ye G (2012) Experimental study on alinite ecocement clinker preparation from municipal solid waste incineration fly ash Mater Struct 45:1145-1153 doi:10.1617/s11527-012-9822-5
34. Wu K, Shi H, Schutter GD, Guo X, Ye G (2012) Preparation of alinite cement from municipal solid waste incineration fly ash Cement and Concrete Composites 34:322-327 doi:10.1016/j.cemconcomp.2011.11.016
35. Wu Y, Xu P, Chen J, Li L, Li M (2014) Effect of Temperature on Phase and Alumina Extraction Efficiency of the Product from Sintering Coal Fly Ash with Ammonium Sulfate Chinese J Chem Eng 22:1363-1367 doi:10.1016/j.cjche.2014.09.008
36. Xu S, Hu H, Guo G, Gong L, Liu H, Yao H (2022) Investigation of properties change in the reacted molten salts after molten chlorides cyclic thermal treatment of toxic MSWI fly ash J Hazard Mater 421:126536 doi:10.1016/j.jhazmat.2021.126536

37. Zeng C, Lyu Y, Wang D, Ju Y, Shang X, Li L (2020) Application of Fly Ash and Slag Generated by Incineration of Municipal Solid Waste in Concrete Adv Mater Sci Eng 2020:1-7 doi:10.1155/2020/7802103
38. Zha X, Hou D, Yu Z, Zhang J, Chou K (2021) Comparison of boundary interpolation methods on the geometrical modeling of viscosity for CaO-Al2O3-SiO2 melts J Non-Cryst Solids 562:120782 doi:10.1016/j.jnoncrysol.2021.120782

Figures

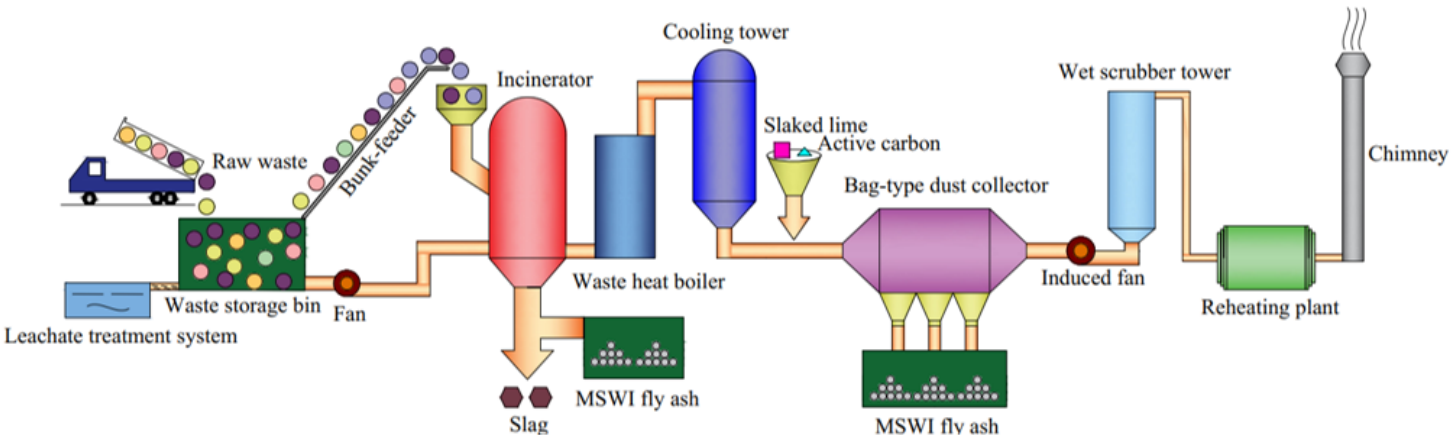

Figure 1

MSWI power plant technological process

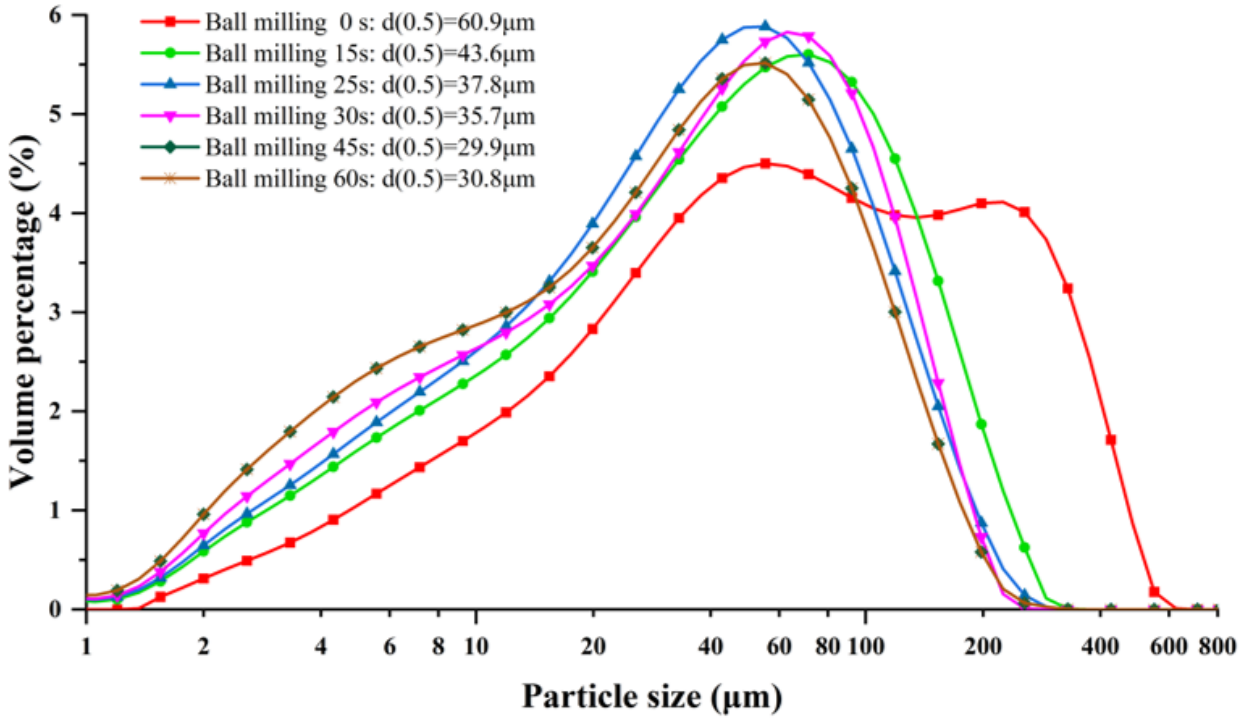

Figure 2

Grain size distribution analysis in different ball milling time

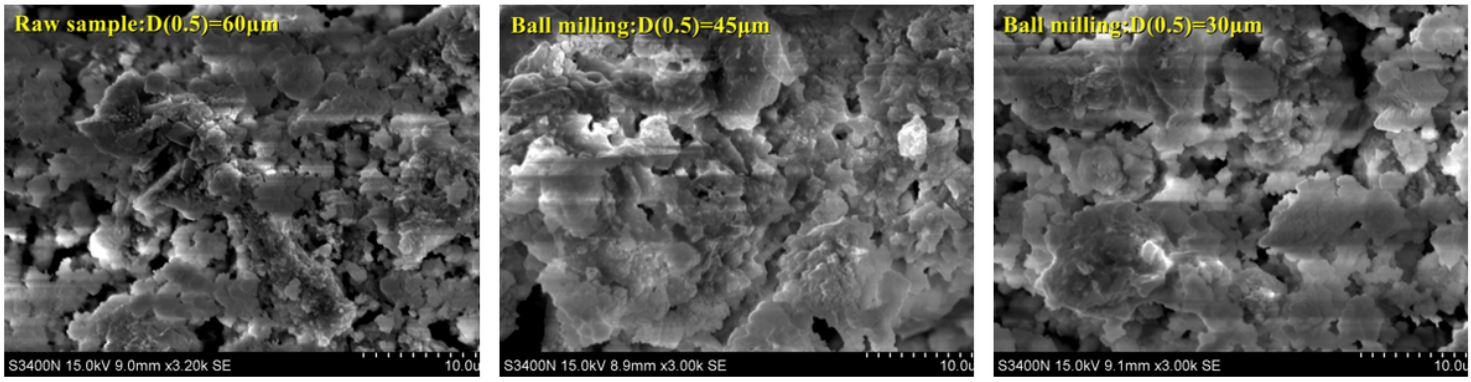

Figure 3

SEM images analysis of raw fly ash in three grain size of D_{50}(60, 45, and 30μm)

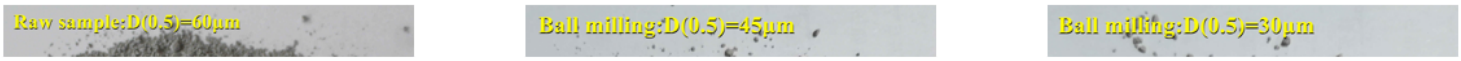

Figure 4

Images for raw fly ash in three grain size of D_{50}(60, 45, and 30μm)

Figure 5

Images for the sintered fly ash in different conditions

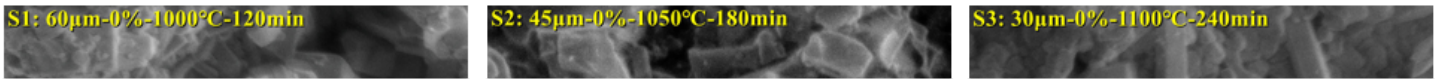

Figure 6

SEM images analysis for sintered fly ash in different conditions

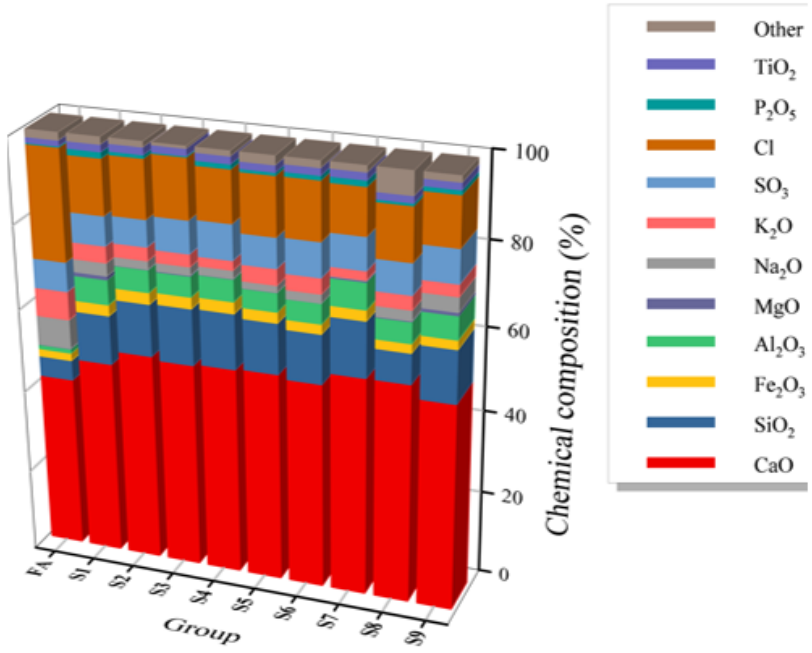

Figure 7

Chemical composition of raw and sintered fly ash in different conditions

Figure 8

XRD analysis results for the raw and sintered fly ash in different conditions

Figure 9

Crystallinity analysis for the raw and sintered fly ash in different conditions

Figure 10

Response surface plots of one factor in grain size of D_{50} for Cr, Cr^{6+}, Ag, and Ba leaching when fluxing agent, setting temperature, and setting time is 2.5%, 1050℃, and 180min, respectively

Figure 11

Response surface plots of one factor in fluxing agent of CaO for Cr, Cr^{6+}, Ag, and Ba leaching when grain size, setting temperature, and setting time is D_{50}=45μm, 1050℃, and 180min, respectively

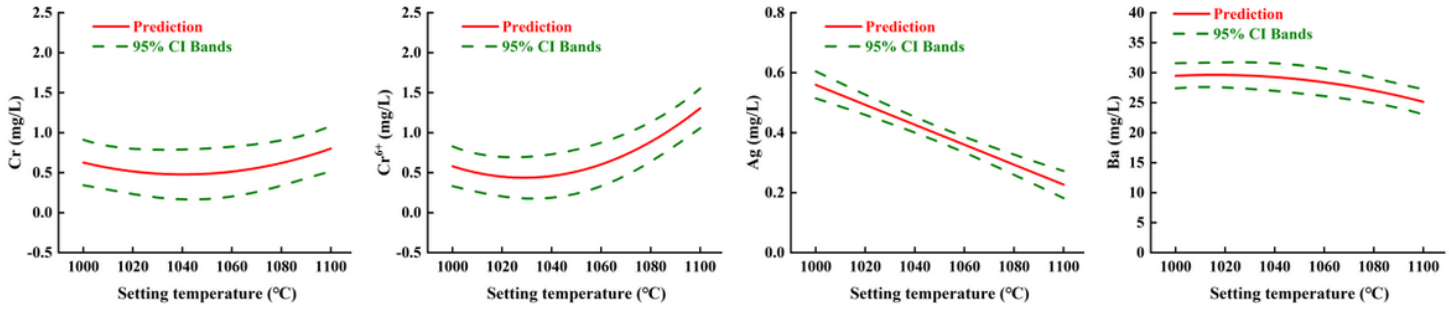

Figure 12

Response surface plots of one factor in setting temperature for Cr, Cr^{6+}, Ag, and Ba leaching when grain size, fluxing agent, and setting time is D_{50}=45μm, 2.5%, and 180min, respectively

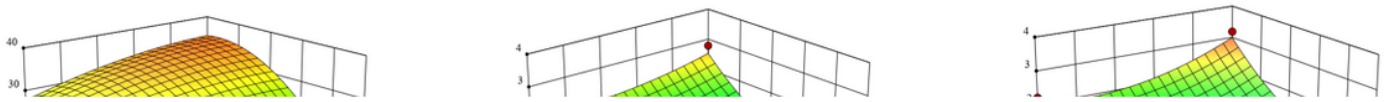

Figure 13

Response surface plots of the interactions between fluxing agent of CaO and setting temperature for Cr, Cr^{6+}, Ag, and Ba leaching

Figure 14

Response surface plots of one factor in setting time for Cr, Cr^{6+}, Ag, and Ba leaching when grain size, fluxing agent, and setting temperature being D_{50}=45μm, 2.5%, and 1050°C, respectively

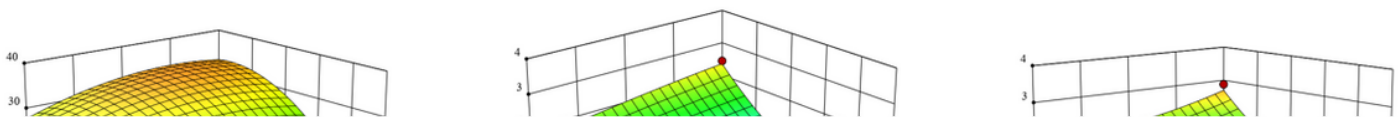

Figure 15

Response surface plots of the interactions between fluxing agent of CaO and setting time for Cr, Cr^{6+}, Ag, and Ba leaching

Figure 16

Main mechanism diagram with leaching characteristic of heavy metals for MSWI fly ash during sintering